Mon. Not. R. Astron. Soc. **000**, 1–10 (2001) Printed 1 February 2008 (MN LaTeX style file v2.2)

Photometry of four binary subdwarf B stars and the nature of their unseen companion stars.

P. F. L. Maxted[1,2], T. R. Marsh[1], U. Heber[3], L. Morales-Rueda[1], R. C. North[1] and W. A. Lawson[4]
[1] *University of Southampton, Department of Physics & Astronomy, Highfield, Southampton, S017 1BJ, UK*
[2] *Department of Physics, Keele University, Staffordshire, ST5 5BG, UK*
[3] *Dr. Remeis-Sternwarte, Astronomisches Institut der Universität Erlangen-Nürnberg, Sternwartstrasse 7, 96049 Bamberg, Germany*
[4] *School of Physics, University College UNSW, Australian Defence Force Academy, Canberra ACT 2600, Australia*

Accepted —; Received —

ABSTRACT

We present lightcurves of four binary subdwarf B stars, Ton 245, Feige 11, PG 1432+159 and PG 1017−086. We also present new spectroscopic data for PG 1017−086 from which we derive its orbital period, $P = 0.073$ d, and the mass function, $f_m = 0.0010 \pm 0.0002 M_{\odot}$. This is the shortest period for an sdB binary measured to-date. The values of P and f_m for the other sdB binaries have been published elsewhere. We are able to exclude the possibility that the unseen companion stars to Ton 245, Feige 11 and PG 1432+159 are main-sequence stars or sub-giant stars from the absence of a sinusoidal signal which would be caused by the irradiation of such a companion star, i.e., they show no reflection effect. The unseen companion stars in these binaries are likely to be white dwarf stars. By contrast, the reflection effect in PG 1017−086 is clearly seen. The lack of eclipses in this binary combined with other data suggests that the companion is a low mass M-dwarf or, perhaps, a brown dwarf.

Key words: binaries: close – stars: horizontal branch – stars: individual: Ton 245 – stars: individual: Feige 11 – stars: individual: PG 1432+159 – stars: individual: PG 1017−086

1 INTRODUCTION

Subdwarf B (sdB) stars dominate surveys for extremely blue stars brighter than B≈16 (Green, Schmidt & Liebert 1986; Downes 1986; Kilkenny et al., 1997). Their effective temperatures ($T_{\rm eff}$ = 20 000K – 40 000K) and surface gravities ($\log g$ = 5.5 – 6.5) place the majority of sdB stars on the extreme horizontal branch (EHB), i.e., they appear in the same region of the $T_{\rm eff} - \log g$ plane as evolutionary tracks for core helium burning stars with core masses of about $0.5 M_{\odot}$ and extremely thin ($\lesssim 0.02 M_{\odot}$) hydrogen envelopes (Heber 1986; Saffer et al. 1994). The extremely low mass of the hydrogen envelope in sdB stars is thought to be due to extensive mass loss when the star was a red giant near the tip of the red giant branch (RGB), i.e., just prior to ignition of helium in the degenerate helium core. If mass loss occurs while the red giant is near the tip of the red giant branch, the core can go on to ignite helium, despite the dramatic mass loss, and may then appear as an EHB star (d'Cruz et al. 1996). The cause of the extensive mass loss has been a matter of some debate, but a recent survey for short period binary EHB stars by Maxted et al. (2001) has shown that in at least 2 out of 3 EHB stars, interactions with companion stars are responsible. In this scenario, the expanding red giant star comes into contact with its Roche lobe and begins to transfer mass to its companion star. This mass transfer is highly unstable, so a "common-envelope" forms around the companion and the core of the red giant. The drag on the companion orbiting inside the common envelope leads to extensive mass loss and dramatic shrinkage of the orbit (Iben & Livio 1993).

The properties of sdB stars, e.g., their orbital period distribution, are a strong test of population synthesis models for binary stars because the common envelope phase which produced the sdB star must have occurred in a star with a degenerate helium core at the tip of the red giant branch. This places useful limits on the mass and radius of the star at the onset of the common envelope phase. Another property of these binaries which can, in principle, be compared to population synthesis models is the relative number of degenerate and non-degenerate companions, i.e., the fraction of sdB stars with main-sequence or sub-giant companions compared to the fraction with white dwarf companions. In this paper we outline a simple method to determine the nature of the companion in practice and apply the method to four sdB binaries with known orbital periods.

2 THE METHOD

In those cases where the companion to an sdB star is not seen directly in the optical spectrum, some other method must be found to determine the nature of the companion star. A sensitive method to detect main-sequence or subgiant companions is to obtain an accurate lightcurve and to look for the effect of the irradiation of one side of the companion star by the hot sdB star. This produces an easily detectable signal with the same period as the orbital period with an approximately sinusoidal shape because the binary appears brightest when we see the irradiated hemisphere face-on and is fainter half an orbit later when we see more of the non-irradiated hemisphere. This sinusoidal distortion to the lightcurve is known as the reflection effect.

2.1 The reflection effect.

It is useful to estimate the amplitude of the reflection effect we expect from a cool, faint companion to an sdB star using the following assumptions and approximations. If the sdB star has an effective temperature T_1 and a radius R_1 the flux intercepted by a companion star of radius R_2 at a distance a, is $\pi R_2^2 \sigma T_1^4 (R_1/a)^2$, where σ is the Stefan-Boltzmann constant. If all of the irradiating flux is re-emitted by the heated face, the effective temperature of the heated face is $T_h \approx T_1(R_1/\sqrt{2}a)^{\frac{1}{2}}$, where we have assumed the intrinsic luminosity of the companion star is negligible. The amplitude of the reflection effect at a given wavelength depends on the spectrum of the sdB star and the spectrum of the reprocessed light from the heated face of the companion star. The spectrum of the reprocessed light we observe will change with orbital phase because the temperature varies across the heated face and the light will not be radiated isotropically from the heated face. The model we describe later takes account of these effects, but for the purposes of estimating the amplitude of the reflection effect we can calculate the maximum flux observed from the heated star using the approximation that it appears as a star of radius R_2 and effective temperature of T_h. For observations at most optical and near-infrared wavelengths, the Rayleigh-Jeans limit of a black body spectrum is a good approximation for the spectrum of the sdB star, i.e, the intensity is proportional to the effective temperature. In the case of strong irradiation, T_h will also be sufficiently high for this approximation to apply to the spectrum of the heated face of the companion.

If we consider a binary which is seen nearly edge-on but is not eclipsing, we find that the difference in magnitudes when we see the irradiated and non-irradiated faces δm, is

$$\begin{aligned}\delta m &\approx 2.5\log_{10}\left[1+\left(\frac{R_2}{R_1}\right)^2\left(\frac{R_1}{\sqrt{2}a}\right)^{\frac{1}{2}}\right]\\ &\approx \left(\frac{R_2}{R_1}\right)^2\left(\frac{R_1}{a}\right)^{\frac{1}{2}} \quad \text{if } \delta\text{m is small}\end{aligned}$$

Although this expression is approximate, it does enable us to estimate the amplitude of the reflection effect we might expect from an sdB star with a main-sequence companion. More importantly, it shows that $\delta m \propto R_2^2$, so a typical white dwarf with a radius of 0.01R$_\odot$ will produce a reflection effect at least 100 times less than a typical M-dwarf with a radius of 0.1R$_\odot$. The actual difference will be much larger than this if the white dwarf is not exceptionally cool but has a more typical effective temperature for white dwarfs of 10–20 000K because the temperature contrast between the heated and unheated hemispheres would then be much less. For example, an sdB star with $T_{\rm eff}$ = 30 000K and a radius of 0.2R$_\odot$ with a cool companion 1R$_\odot$ distant (P$\sim$ 4 h) will show a reflection effect of about 0.1 magnitudes, which is easily detectable with differential CCD photometry. By contrast, a white dwarf with a radius of 0.01R$_\odot$ at the same distance gives rise to a reflection effect of no more than 0.001 magnitudes. Even if the inclination of the binary reduced the amplitude of the reflection effect by an order of magnitude, it would be straightforward to distinguish the nature of the companions in these two hypothetical binary sdB stars using the presence or absence of a reflection effect in the lightcurve.

2.2 Our model.

We have used a simple model to produce synthetic lightcurves for the sdB binaries we have observed which is based on numerical integration over the visible surface of the heated star. The visible surface of the irradiated star is defined by a Roche potential. The effective temperature at the integration points on the heated face, T_h' is calculated from $T_h' = (T_u^4 + f'/\sigma)^{1/4}$, where T_u is the mean effective temperature of the unheated face and f' is the irradiating flux over that region of the star allowing for the angle between the normal to the surface and the direction of the sdB star. The other parameters of our model are the radius of the sdB star in units of the orbital separation, r_1; the radius of the companion star in units of the distance between its centre and the inner Lagrangian point measured along the same axis (the filling-factor), f; the inclination of the orbit, i; the mass ratio, $q = M_2/M_1$; the orbital period, P, the effective temperature of the sdB star, T_1. The observed flux at a given wavelength and orbital phase can then be estimated by assuming that both stars radiate as black-bodies. We also include limb darkening and gravity darkening in the calculation of the reflection effect. The details of the treatment of these effects in our model has a negligible effect on the predicted amplitude of the reflection effect so we do not describe them here. Our model does not include any contribution to the lightcurve due to the distortion of the sdB star by its companion, i.e, the ellipsoidal effect from the sdB star is ignored. This effect is negligible for Ton 245, Feige 11 and PG 1432+159 but not for PG 1017−086.

Our calculation of the effective temperature over the surface of the companion star is equivalent to assuming that the bolometric albedo of the companion star, α, is 1. There is good observational evidence for cool companions to hot subdwarf stars having high bolometric albedos, at least for short period binaries. For example, Drechsel et al. (2001) have presented B and R lightcurves of the eclipsing sdB star HS 0705+6700 which has an M-dwarf companion and an orbital period of $P = 2.3h$. They used the Wilson-Devinney code (Wilson & Devinney 1971) to model the lightcurve and found that to achieve satisfactory fits to the lightcurves a value of $\alpha = 1$ is required. The fits were improved by using a value of $\alpha = 1.1$, which is unrealistic and is a consequence of using a monochromatic lightcurve model based on black body radiation to model a broad band lightcurves

of an irradiated star whose spectrum is certainly very different to a black body. Our model is also affected by this problem. Similarly, Hilditch, Harries & Hill (1996) analysed the lightcurves of HW Vir, KV Vel (sdO+M, P=8.6h) and AA Dor (sdO+M, $P = 6.3h$) with the lightcurve model LIGHT2 (Hill & Rucinski 1993) and also found $\alpha = 1$ or more is required to reproduce the reflection effect. Wood, Zhang & Robinson (1993) confirmed the requirement for a high albedo in HW Vir by using the Wilson-Devinney code to analyse their UBVR lightcurves of HW Vir.

Although our model is quite simple, it is able to predict the amplitude of the reflection effect in sdB binaries with faint companions with an accuracy of about 50 percent. To demonstrate this, we have calculated the amplitude of the reflection effect for two sdB stars with faint companions, HW Vir and PG 1336−018 and the sdOB binary V477 Lyr. These three stars are eclipsing binaries so the properties of the stars can be determined independently. This is shown in Table 1, where we compare the observed amplitude of the reflection effect in the V and I bands, δV and δI, to the value calculated using our model. We also list the properties of each binary in Table 1 which have the greatest effect on the values of δV and δI predicted by our model. In all three cases we see that the amplitude in the V band is predicted correctly to within 50 percent. For HW Vir where the amplitude has also been measured in the I-band, the amplitude predicted by our model agrees very well with the observed value.

3 OBSERVATIONS AND REDUCTIONS

3.1 Photometry

We used the 1m Jacobus Kapteyn telescope (JKT) on the Island of La Palma to obtain V images and I band images of PG 1432+159 (57 V images, 52 I images), Feige 11 (80 V images, 85 I images) and Ton 245 (29 V images, 40 I images) on the nights 1998 Aug 2–10. Additional observations of Ton 245 (9 V images, 9 I images) were acquired on the night 1999 Jan 3. The detector used was a TEK charged-coupled device (CCD) with 1024^2 pixels giving an image scale of $0.34''$ per pixel. Exposure times varied between 10s and 120s and the deadtime between exposures was 60s. We obtained 40 V band images of PG 1017−086 with the same telescope using a SITe CCD with 2048^2 pixels giving an image scale of $0.34''$ per pixel on the night 2001 May 3. The exposure times were 70s or 100s and the deadtime between exposures was 110s. We also acquired 45 V band images of PG 1017−086 with the SAAO 1m telescope using a SITe CCD with 1024^2 pixels giving an image scale of $0.31''$ per pixel on the night 2001 May 7. The exposure time was 90s and the deadtime between exposures was 73s.

The bias level in every image was determined from the overscan regions and was subtracted from the image before further processing. Images of the twilight sky devoid of any bright stars were used to determine flat-field corrections by forming the median image of 3–5 twilight sky images in each filter, one for each night's data. We used optimal photometry (Naylor 1998) to determine instrumental magnitudes of the stars in each frame. We checked for variability in the stars other than the target star in each frame before calculating differential magnitudes between the target star and the total flux in the comparison stars. The positions and approximate V magnitudes of the targets and comparison stars are given in Table 2. The coordinates and identification numbers (in parentheses) in Table 2 were taken from Guide Star Catalogue-II [1]. We have used published Strömgren y magnitudes for PG 1432+159 and PG 1017−086 in place of V, the difference for these blue stars are small ($\lessapprox$ 0.05mag). The magnitude of the comparison stars given in Table 2 was calculated from the published target magnitude given and the median magnitude difference from our own photometry.

Table 2. Position and magnitudes of the target and comparison stars used for our differential photometry.

Target	α(J2000)	δ(J2000)	V	Ref.
Ton 245	15 40 35.4	+26 47 42	13.89	1
(N1330313366)	15 40 43.1	+26 46 52	15.79	
(N133031310095)	15 40 37.4	+26 48 21	18.17	
(N133031310109)	15 40 32.5	+26 48 43	17.36	
Feige 11	01 04 21.7	+04 13 37	12.06	2
(N320132243)	01 04 28.0	+04 11 55	14.47	
(N320132247)	01 04 28.4	+04 11 25	13.80	
PG 1432+159	14 35 19.2	+15 40 14	13.90	3
(N1313121947)	14 35 16.0	+15 39 59	15.94	
(N1313121769)	14 35 13.7	+15 36 41	15.61	
(N1313121359)	14 35 11.9	+15 36 45	14.82	
(N13131213083)	14 35 26.3	+15 39 17	16.55	
PG 1017−086	10 20 14.5	−08 53 46	14.43	3
(S1212232199)	10 20 08.5	−08 50 58	13.11	

1. Iriarte (1959); 2. Landolt (1983); 3. Wesemael et al. (1992).

3.2 Spectroscopy

We obtained low-resolution spectra of Ton 245 using the red arm of the ISIS double beam spectrograph on the 4.2m William Herschel Telescope on the Island of La Palma on the night 2001 February 22. We also obtained spectra with the same instrument of the K3V star GL 250 A and the M1.5V star GL 220. We used a 158 line/mm grating and a TEK CCD with a 1 arcsec wide slit to obtain spectra with a resolution of 5–6Å and a mean dispersion of 2.9Å/pixel. We applied a flux calibration to these spectra using observations of G191−B2B and the tabulated fluxes of Oke (1990). We have made no correction for slit-losses in this calibration.

We observed PG 1017−086 using with the 2.5m Isaac Newton Telescope on the Island of La Palma. A total of 22 spectra were acquired on the nights 2000 April 11, 2001 March 8–11 and 2001 May 6. Spectra were obtained with the

[1] The Guide Star Catalogue-II is a joint project of the Space Telescope Science Institute and the Osservatorio Astronomico di Torino. Space Telescope Science Institute is operated by the Association of Universities for Research in Astronomy, for the National Aeronautics and Space Administration under contract NAS5-26555. The participation of the Osservatorio Astronomico di Torino is supported by the Italian Council for Research in Astronomy. Additional support is provided by European Southern Observatory, Space Telescope European Coordinating Facility, the International GEMINI project and the European Space Agency Astrophysics Division.

Table 1. The observed amplitude of the reflection effect in HW Vir, PG 1336-018 and V477 Lyr and the amplitude calculated from our model.

Name	P(d)	Spec. Type	T_1(K)	M_1	q	$i(^\circ)$	f	r_1	δV Obs.	δV Cal.	δ I Obs.	δ I Cal.	Ref.
HW Vir	0.117	sdB+M	28500	0.5	0.3	81	0.34	0.205	0.26	0.24	0.30	0.30	1,2
PG 1336-018	0.101	sdB+M5	33000	0.5	0.3	81	0.53	0.19	0.20	0.27	—	—	3
V477 Lyr	0.471	sdOB+M	60000	0.51	0.29	80.5	0.54	0.077	0.78	0.65	—	—	4

1. Wood & Saffer (1999); 2. Kiss et al. (2000); 3. Kilkenny et al. (1998); 4. Pollacco & Bell (1994);

intermediate dispersion spectrograph using the 500mm camera, a 1200 line/mm grating and a TEK CCD as a detector. The spectra cover 400Å around the Hα line at a dispersion of 0.39Å per pixel. The slit width used was 0.97 arcsec which gave a resolution of about 0.9Å. The exposure time per spectrum was 600s or 900s. We also obtained a continuous series of 26 spectra of PG 1017−086 on the night 2001 March 12 using the 235mm camera, a 900 line/mm grating and an EEV CCD. The spectra cover the wavelength range 3700 – 5400Å at a dispersion of 0.63Å per pixel with a resolution of about 1.6Å and the exposure time per spectrum was 300s.

We extracted the spectra from the images using optimal extraction to maximize the signal-to-noise (Marsh 1989). We observed arcs before and after all observations of PG 1017−086. The arcs associated with each stellar spectrum were extracted using the same weighting determined for the stellar image to avoid possible systematic errors due to the tilt of the spectra on the detector. The wavelength scale was determined from a fit to measured arc line positions and in each case the standard deviation of the fit is much less than 1 pixel. The wavelength scale for an individual spectrum was determined by interpolation to the time of mid-exposure from the fits to arcs taken before and after the spectrum to account for the small amount of drift in the wavelength scale due to flexure of the instrument. Statistical errors on every data point calculated from photon statistics are rigorously propagated through every stage of the data reduction.

4 PG 1017−086

4.1 Radial velocities

We first observed PG 1017−086 as part of a survey for binary sdB stars (Maxted et al. 2001). The two spectra we obtained for that survey showed a change in radial velocity measured from the Hα line of about 60km s^{-1} over half an hour. We obtained further observations of the Hα line of PG 1017−086 to determine the orbital period and mass function. To measure the radial velocity we used least-squares fitting of a model line profile. This model line profile is the summation of three Gaussian profiles with different widths and depths but with a common central position which varies between spectra. Only data within 2000 km s^{-1} of the Hα line is included in the fitting process and the spectra are normalized using a linear fit to the continuum either side of the Hα line. We used a least-squares fit to one of the spectra to determine an initial shape of the model line profile. A least squares fit of this profile to each spectrum in which the position of the line is the only free parameter gives an initial set of radial velocities. We used these initial radial velocities to fix the position of the Hα line in a simultaneous fit to all the spectra to obtain an improved model line profile. A least squares fit of this profile to each spectrum yields the radial velocities given in Table 3 and are labeled “Red”. A similar process was used to measure radial velocities from the Hβ – Hϵ lines with two Gaussian profiles used to model each line. These are given in Table 3 and are labeled “Blue”. The uncertainties quoted are calculated by propagating the uncertainties on every data point in the spectra right through the data reduction and analysis.

The periodogram of the radial velocities given in Table 3 shows a single unambiguous orbital frequency at 13.70 cycles/day. We used a least-squares fit of a sine wave of the form $\gamma + K\sin((T - T_0)/P)$ to obtain the parameters given in Table 4, where γ is the systemic velocity, K is the projected orbital speed, T is the time of mid-exposure of the spectrum and P is the orbital period. The measured radial velocities are shown in Fig. 1 as a function of orbital phase together with the sine wave determined from the least-squares fit.

We rebinned all the spectra near Hα onto a common wavelength scale allowing for the measured radial velocity shifts and then formed the average spectrum, and similarly for the spectra of the bluer Balmer lines. There are no spectral features attributable to a cool companion star visible in either of these average spectra. We used the average blue spectrum to measure the effective temperature, $T_{\rm eff}$, the surface gravity $\log g$ and the helium abundance by number, y, by fitting model spectra to the Balmer lines (Hβ to H 10), the He I lines (4026Å, 4388Å, 4471Å, 4713Å, 4922Å) and He II 4686Å lines using the procedure outlined in Saffer et al. (1994). We used the synthetic spectra derived from H and He line blanketed NLTE model atmospheres of Napiwotzki (1997). We find $T_{\rm eff} = 30300 \pm 80$K, $\log g = 5.61 \pm 0.02$ and $y = 0.0016 \pm 0.0001$ from these fits, where the uncertainties are “internal errors” from the fitting procedure and do not include uncertainties in the models themselves. The spectrum and fit are shown in Fig. 2. The synthetic spectra were convolved beforehand with a Gaussian profile of the appropriate width to account for the instrumental profile and with a broadening function to account for a projected rotational velocity, $V_{\rm rot}\sin i$, of 118km s^{-1}. This was determined from a least-squares fit to the Hα line of a synthetic line profile for the appropriate $T_{\rm eff}$, $\log g$ and y values convolved with a broadening function for various values of $V_{\rm rot}\sin i$. From a plot of χ^2 versus $V_{\rm rot}\sin i$ we estimate a value of $V_{\rm rot}\sin i$=118 $^{+7}_{-4}$km s^{-1}. The radius of a 0.5M$_\odot$ sdB star with $\log g$=5.61 is 0.19M$_\odot$. If we assume tidal forces have forced the sdB star to co-rotate with the binary, the rotational velocity of the sdB star is 132km s^{-1}. The measured

Table 3. Measured heliocentric radial velocities for PG 1017−086.

HJD−2450000	Radial velocity ($\mathrm{km\,s^{-1}}$)	Spectrum
1646.4502	-63.4 ± 7.1	Red
1646.4614	-1.9 ± 6.4	Red
1977.4525	-27.7 ± 12.3	Red
1977.4595	-25.4 ± 12.0	Red
1977.4665	-36.9 ± 13.2	Red
1977.4735	-54.1 ± 10.9	Red
1978.5806	-31.5 ± 8.2	Red
1978.5910	30.9 ± 9.3	Red
1979.5198	-60.5 ± 6.6	Red
1979.5302	-13.3 ± 6.3	Red
1979.5786	-53.4 ± 7.2	Red
1979.5891	-49.6 ± 7.0	Red
1980.4757	-37.7 ± 7.1	Blue
1980.4793	-12.0 ± 7.2	Blue
1980.4829	-6.2 ± 7.4	Blue
1980.4864	23.6 ± 7.5	Blue
1980.4900	25.8 ± 7.0	Blue
1980.4936	42.1 ± 6.4	Blue
1980.4971	43.1 ± 6.5	Blue
1980.5007	38.6 ± 6.7	Blue
1980.5043	42.1 ± 6.9	Blue
1980.5078	27.4 ± 6.8	Blue
1980.5129	15.3 ± 7.0	Blue
1980.5164	-5.5 ± 6.9	Blue
1980.5200	-29.6 ± 7.0	Blue
1980.5236	-40.3 ± 7.0	Blue
1980.5272	-48.2 ± 6.7	Blue
1980.5307	-54.1 ± 6.6	Blue
1980.5343	-67.6 ± 6.7	Blue
1980.5379	-44.0 ± 6.5	Blue
1980.5414	-53.6 ± 6.6	Blue
1980.5450	-59.9 ± 6.7	Blue
1980.6119	-49.6 ± 7.0	Blue
1980.6155	-45.2 ± 6.5	Blue
1980.6191	-32.5 ± 6.6	Blue
1980.6226	-21.9 ± 7.2	Blue
1980.6262	-22.6 ± 7.6	Blue
1980.6298	1.3 ± 7.4	Blue
2036.3872	-26.6 ± 25.7	Red
2036.3948	-3.7 ± 21.5	Red
2036.4024	6.1 ± 14.9	Red
2036.4100	28.2 ± 13.6	Red
2036.4180	37.9 ± 15.6	Red
2036.4256	3.1 ± 14.4	Red
2036.4332	-20.9 ± 17.6	Red
2036.4407	-46.5 ± 19.6	Red
2036.4483	-57.6 ± 44.0	Red

value of $V_{\mathrm{rot}} \sin i$ would then imply that the inclination of the binary is $63^\circ\,^{+8^\circ}_{-4^\circ}$.

4.2 The lightcurve and the nature of the companion

Our photometry of PG 1017−086 is shown in Fig. 3 as a function of the orbital phase calculated from the values of T_0 and P derived above. The reflection effect with an amplitude of about 0.08 magnitudes can be clearly seen and maximum light is at phase zero as expected, i.e., when the sdB star is closest to the observer. The difference between the mean level of the lightcurves observed with the SAAO 1m telescope and the JKT is due to a difference in the sensitivity of the CCDs used at the bluest wavelengths passed by the V filter. This makes PG 1017−086 appear brighter than its redder comparison star for the CCD with better blue sensitivity.

Figure 1. Radial velocities of PG 1017−086 measured from the Hα line (open circles) and from the Hβ – Hϵ lines (closed circles). The sine wave fit described in the text is also shown (solid line).

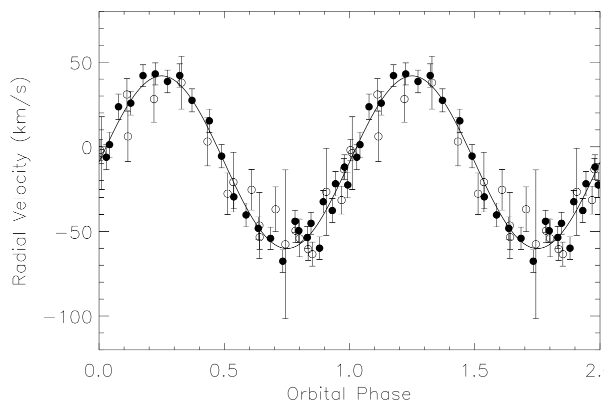

Table 4. Circular orbit fit to the measured radial velocities for PG 1017−086.

T_0 (HJD)	2452036.3940 ± 0.0005
P (days)	0.0729938 ± 0000003
γ($\mathrm{km\,s^{-1}}$)	−9.1 ± 1.3
K($\mathrm{km\,s^{-1}}$)	51.0 ± 1.7
χ^2	46.1
N	47

The minimum mass of the companion to a $0.5\mathrm{M}_\odot$ sdB star for the values of P and K observed in PG 1017−086 is $0.0687{\pm}0.025\mathrm{M}_\odot$. The mass of the companion for the inclination of $63^\circ\,^{+8^\circ}_{-4^\circ}$ calculated above is $0.078\,^{+0.005}_{-0.006}\,\mathrm{M}_\odot$. If we assume the companion is a low mass M-dwarf with a typical radius of $0.085\mathrm{R}_\odot$, we find that our simple model for the reflection effect predicts an amplitude for the lightcurve of 0.074 magnitudes, which is consistent with the amplitude observed (Fig. 3) given the uncertainties involved, i.e., about 50 percent. The amplitude of the reflection effect seen in the lightcurve cannot be produced by a white dwarf companion. The lack of any eclipse sets an upper limit to the inclination of 72° for the radius of sdB star we have calculated. The limit reduces to 63° if we assume the companion has a radius of $0.085\mathrm{R}_\odot$, which is consistent with the inclination used in the calculation of the reflection effect. Our model does not include the ellipsoidal effect due to the sdB star, which is expected to be about 0.01 magnitudes. This is too small to be measured reliably from our lightcurves, but would be measurable with improved data, particularly at bluer wavelengths where the sdB star dominates. The size of the ellipsoidal effect depends strongly on the size of the star relative to its Roche lobe, so this measurement would usefully constrain the properties of the stars in PG 1017−086.

In summary, we can say the companion to PG 1017−086 is a low mass star or, perhaps, a brown dwarf, but is certainly not a white dwarf star.

Figure 2. Synthetic spectrum fit to the blue Balmer lines and helium lines of PG 1017−086

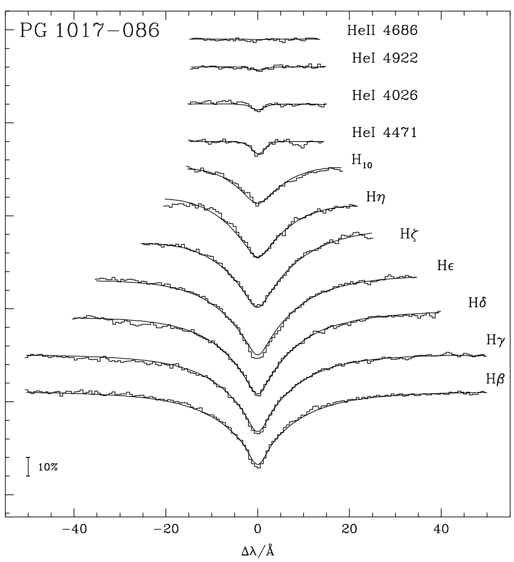

Figure 3. The V-band lightcurve of the PG 1017−086 observed with the SAAO 1m telescope (filled circles) and with the JKT (open circles). The solid lines are cosine functions with an amplitude of 0.083 magnitudes

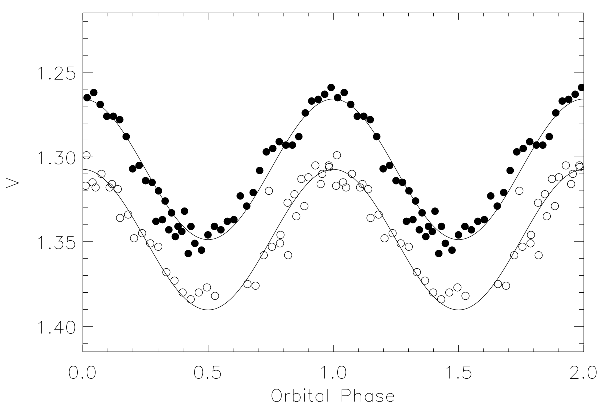

5 TON 245, FEIGE 11 AND PG 1432+159

In this section we have to go through a fairly complex chain of logic in order to establish the final result, which is that the companions of the three stars Ton 245, Feige 11 and PG 1432+159 must all be compact as opposed to main-sequence stars or brown dwarfs. To help the reader, we now give an overview of the reasoning we employ.

We detect no significant reflection effect in any of these stars and our task is to show that this is enough to say that they must have compact companions, most likely white dwarfs. The complicating factor is the unknown orbital inclination which also affects the reflection effect amplitude in the sense that the amplitude becomes small as orbits become more face-on. In fact the reflection amplitude can also decrease at *high* inclinations because for a given radial velocity amplitude a high inclination implies a reduced companion star mass which, in turn, implies a reduced radius and, therefore, a reduced reflection effect. However it is the reduction at low inclinations that is much more significant, e.g., see Fig. 6. This essentially means that very low mass companions are ruled out by the radial velocity amplitudes and therefore we cannot get a small reflection effect by appealing to brown dwarf companions for these three stars. Thus, the problem boils down to ruling out low inclinations as a way of getting low amplitudes. We can do so as follows:

From spectra of the targets we can place upper limits upon the contribution of the companion stars to the sdB spectra. Given the luminosity of the sdB stars at that wavelength, the main-sequence mass-luminosity relation implies upper limits upon the companion star masses. For a given sdB mass, radial velocity amplitude and orbital period, an *upper* limit on the companion mass gives a *lower* limit upon the inclination (see Fig. 6). This in turn gives a lower limit upon the predicted amplitude of the reflection effect on the assumption of main-sequence companions. The loop is finally closed when we establish that this lower limit should have been detectable in each case, and therefore that the companions must be compact.

5.1 Upper limits to the luminosity ratios.

In order to set upper limits on the contribution from any cool companion star to the spectra of Ton 245, Feige 11 and PG 1432+159, we have considered a region of the spectrum where we expect to see no features from the sdB star or the Earth's atmosphere. We then subtract off varying amounts of cool star spectrum to find the luminosity ratio at which the combined spectrum no longer looks featureless, i.e., for which a low-order polynomial is no longer a good fit.

For Feige 11 and PG 1432+159 we used the average spectra near Hα described in Moran et al. (1999). We compared these spectra to a spectrum of GL 69, a K5V star. All the spectra were shifted in wavelength so that spectral features appear at their rest wavelengths and then rebinned onto uniform wavelength grid of 215 elements between 6365Å and 6450Å. There are no significant spectral features from the sdB star or the Earth's atmosphere in this wavelength region. The spectra were normalized to give a continuum value of 1. We then calculated the χ^2 statistic for a least-squares parabolic fit to the residual $f_{sdB} - L \cdot f_{GL69} + L$ where f_{sdB} and f_{GL69} are the normalised spectra of the sdB star and GL 69 respectively. The results are shown as a function of the luminosity ratio, L, in Fig. 4.

If χ^2_0 is the value of χ^2 for $L = 0$, then we can set an upper limit to L by considering the minimum value of L for which χ^2 is significantly worse than χ^2_0. We have chosen a conservative value of $\chi^2_0 + 3$ (91.6 percent confidence limit) and find corresponding upper limits of $L < 0.0026$ for Feige 11 and $L < 0.009$ for PG 1432+159.

We applied the same technique to our low-resolution ISIS spectrum of Ton 245 and the K3V GL 250 A in the spectral region 8350Å to 8600Å, which is also free of spectral features from the sdB stars or the Earth's atmosphere. The rebinned spectra have 86 pixels in this case. The results are shown in Fig. 4 where it can be seen that $L < 0.043$. The limit on L is less stringent than those calculated for Feige 11 or PG 1432+158 because there are fewer spectral features visible at lower resolution. We also applied the technique to

Ton 245 and the M1.5V star GL 220 and found $L < 0.046$. Although the value of χ^2 is slightly improved by subtracting 1–2 percent of a cool star spectrum from the spectrum of Ton 245, this is not a significant improvement and it is likely to be due to the cancellation of flat-fielding errors, sky subtraction problems and weak absorption features due to the Earth's atmosphere rather than any real detection of a cool companion.

5.2 The amplitude of the reflection effect from a main-sequence companion

In order to calculate the amplitude of the reflection effect from a main-sequence and the luminosity ratio as a function of inclination, we proceed as follows. For a given orbital inclination, the semi-amplitudes and orbital periods given in Table 6 can be used to compute the mass of the companion star and the separation of the stars assuming a mass of $0.5\mathrm{M}_{\odot}$ for the sdB star. The radius of the sdB star can be estimated using the surface gravity given by Saffer et al. (1994). The radius, effective temperature and absolute visual magnitude of the companion star can be estimated from its mass using the tabulations of Zombeck (1990). We can then use our model for the reflection effect to predict the amplitude of the reflection effect as a function of the inclination. The luminosity ratio in the V-band can also be calculated given the absolute visual magnitude of the sdB star calculated from the radius and effective temperature of the sdB star combined with a surface brightness in the V band from the model atmospheres described above. The results of these calculations are shown in Fig. 6. We can see from the right-hand panels of Fig. 6 that the upper limit to the luminosity ratio calculated above sets a lower limit to the inclination of the binary if we assume the companion is a main-sequence star. Although the luminosity ratio was calculated at redder wavelengths than the V-band, the cool companion is redder than the sdB star at these wavelengths, so this is a pessimistic assumption, i.e., we allow a greater range of inclinations by applying these upper limits calculated from the spectra to the V-band. In Table 6 we list the minimum amplitude of the reflection effect predicted by our model for the range of inclinations allowed by the upper limit to luminosity ratio, $\delta m_{\rm min}$.

5.3 The observed lightcurves

The lightcurves of Ton 245, Feige 11 and PG 1432+159 are shown in Fig. 5. Also shown are the results of a least-squares fit of a cosine wave to these data with the same period as the orbital period. The amplitude of these cosine waves, δm, is given in Table 5 together with the standard deviation of the residuals, $\sigma_{\delta m}$. We have also calculated periodograms for each lightcurve, i.e,. the semi-amplitude of sine wave fit by least squares as a function of frequency. The results are shown in Fig. 7. Almost all the power in these periodograms occurs near 1 cycle/day or its aliases and is due to a combination of the window function and differential extinction between the target and comparison stars. It is clear that there is no significant variability in these lightcurves with the same period as the orbital period and that any reflection effect in these binaries has an amplitude less than about 0.01 magnitudes. We compare these measured semi-amplitudes to the minimum semi-amplitudes for the reflection effect from a main-sequence calculated above by calculating the ratio $(\delta m_{\rm min} - \delta m)/\epsilon_{\delta m}$, where $\epsilon_{\delta m}$ is the uncertainty in δm. We see that in all three cases the minimum predicted semi-amplitude exceeds the observed semi-amplitude by an order-of-magnitude more than its uncertainty.

We have also considered the sources of uncertainty in our analysis. The uncertainties in the properties of the sdB star, i.e., mass, radius and temperature, affect the value of $\delta_{\rm min}$ by no more than a few hundredths of a magnitude. Another source of uncertainty is the scatter in the mass-radius relation for M-dwarfs, which is about 12% (Caillault & Patterson 1990), but this also has a small effect on $\delta_{\rm min}$. The largest source of uncertainty in our analysis is the error introduced by the assumptions and approximations used in our model of the reflection effect. These are difficult to quantify but we have shown that for sdB binaries similar to those we are studying but with M-dwarf companions, the model is able to predict the amplitude of the reflection effect to within 50 percent. Even if we are pessimistic and assume that the uncertainties in the models used to derive $\delta m_{\rm min}$ are a factor of a few, it is clear that the amplitude of any reflection effect in the lightcurves of Ton 245 are a factor of at least ~ 4 lower than that expected from a main-sequence companion and are an order-of-magnitude lower for the lightcurves of Feige 11 and PG 1432+159.

There is no evidence in any of our lightcurves of variability on timescales of 90s – 600s, which is the typical period range for pulsating sdB stars (Koen et al. 1999). However, our data are far from ideal for studying pulsations given the long exposure times used and poor data sampling so it is quite possible that one or more of the stars studied are pulsating sdB stars.

6 DISCUSSION

We can rule out the possibility that the companions to Ton 245, Feige 11 and PG 1432+159 are main-sequence stars because they do not show any reflection effect in their lightcurves. We can also rule out a sub-giant companion in all three cases because a sub-giant is, by definition, larger than a main-sequence star, so the reflection effect would be much larger. We conclude that none of these sdB stars has a main-sequence or sub-giant companion. The companions to these sdB stars have masses $\gtrsim 0.3\mathrm{M}_{\odot}$ but must have radii much smaller than main-sequence stars to avoid the reflection effect being seen in the lightcurve. A white dwarf companion satisfies these constraints comfortably and sdB – white dwarf binaries are known to exist, e.g., KPD 0422+5421 (Koen, Orosz & Wade 1998), KPD 1930+2752 (Maxted et al. 2000).

The orbital period we have measured for PG 1017−086 is the shortest period for an sdB binary measured to-date and is comparable to those of short-period cataclysmic variables. The timescale for orbital shrinkage due to the loss of gravitational waves is about 800 Myr, which is comparable to the lifetime of an sdB star. It is interesting to speculate what the binary will look like if mass transfer begins before the sdB star evolves into a low mass white dwarf. The stream of material from the M-dwarf will impact directly

Figure 4. The upper limits to the luminosity ratio, L, for Ton 245, Feige 11 and PG 1432+159. The panels on the left show the χ^2 statistic for a least-squares fit of a parabola to the residuals after subtracting a fraction L of a cool star spectrum from the observed spectrum of the sdB star. The value of the χ^2 statistic for $L = 0$, χ^2_0 is show by a horizontal solid line and the value χ^2_0+3 which sets the upper limit to L is shown with a horizontal dashed lines. The panels on the right show spectra of Feige 11 and PG 1432+159 together with the spectrum of the K5V star GL 69 offset by -0.2 for clarity and similarly for Ton 245 and the K3V star GL 250 A.

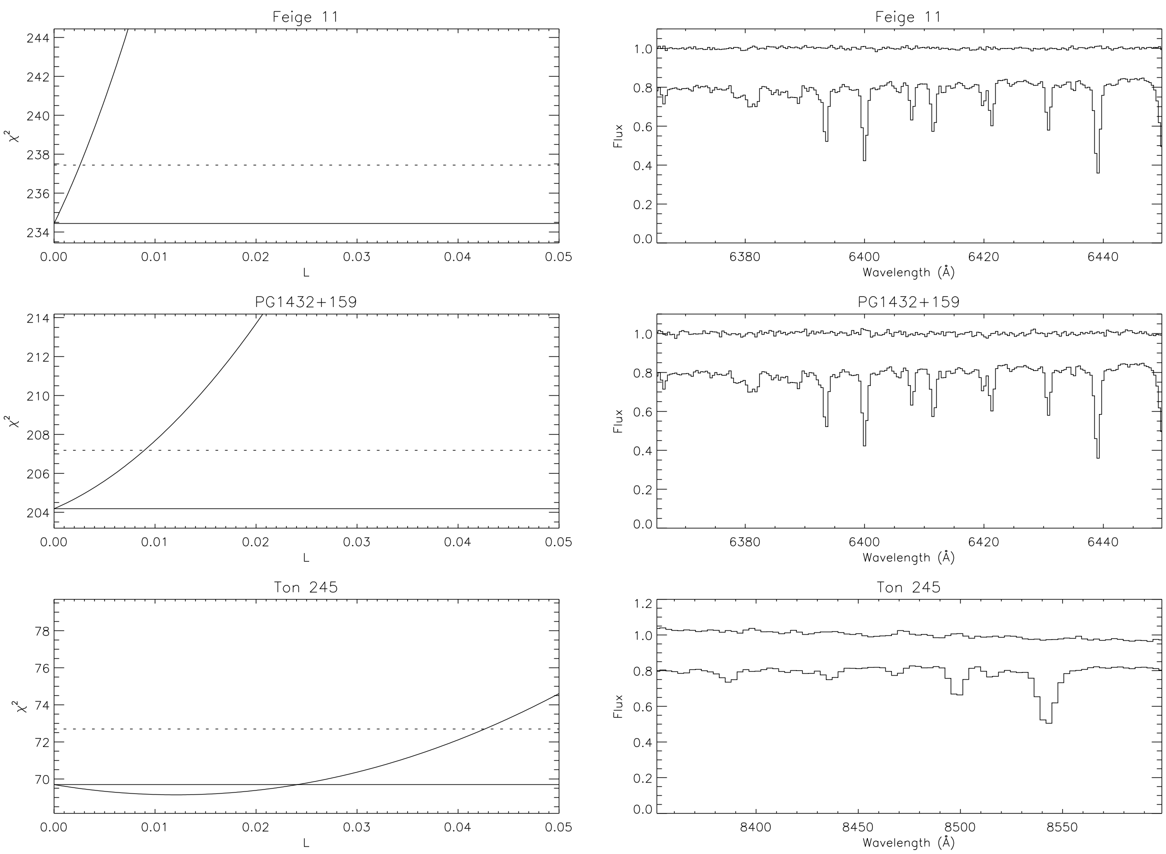

Table 5. Cosine fits to our V and I lightcurves. The amplitude of the cosine, δm, and the standard deviation of the residuals, $\sigma_{\delta m}$, are given in magnitudes with the number of observations given in parentheses. The figure in the final column is the ratio of $(\delta m_{\rm min} - \delta m)/\epsilon_{\delta m}$, where $\epsilon_{\delta m}$ is the uncertainty in δm.

Name	Filter	δm	$\sigma\delta m$	$\frac{(\delta m_{\rm min}-\delta m)}{\epsilon_{\delta m}}$
Ton 245	V	0.0050	0.0081	10.9
		±0.0038	(n=38)	
	I	0.0088	0.0137	19.5
		±0.0056	(n=49)	
Feige 11	V	0.0162	0.0187	46.4
		±0.0060	(n=80)	
	I	0.0162	0.0192	88.3
		±0.0058	(n=85)	
PG 1432+159	V	0.0104	0.0127	90.3
		±0.0048	(n=57)	
	I	0.0164	0.0175	91.1
		±0.0070	(n=52)	

onto the surface of the sdB star, i.e., no accretion disk will form, so the effects of the mass transfer may not be immediately obvious.

7 CONCLUSION

We have presented lightcurves in two colours of three binary subdwarf B stars – PG 1432+159, Feige 11 and Ton 245. We have shown that there is no sign in these lightcurves of the sinusoidal variation which would be seen if the companion star were a main-sequence star or a sub-giant. The most likely explanation is that all three sdB stars have white dwarf companion stars.

By contrast, the reflection effect in PG1017−086 is clearly seen in the lightcurve. We have presented spectroscopy of this star from which we have measured the orbital period, mass function and projected rotational velocity. These observations show that PG1017−086 is an sdB star with a low-mass M-dwarf or brown dwarf companion.

ACKNOWLEDGMENTS

PFLM was supported by a PPARC post-doctoral grant. The Jacobus Kapteyn Telescope is operated on the island of La Palma by the Isaac Newton Group in the Spanish Observatorio del Roque de los Muchachos of the Instituto de Astrofisica de Canarias. The SAAO is a National Facility administered by the National Research Foundation of South Africa.

Figure 5. Lightcurves in V and I of Ton 245, Feige 11 and PG 1432+159. The points mark the magnitude of the target relative to the total flux in the companion stars listed in Table 2. Least-squares fits of a cosine with the same period as the orbital period are also shown.

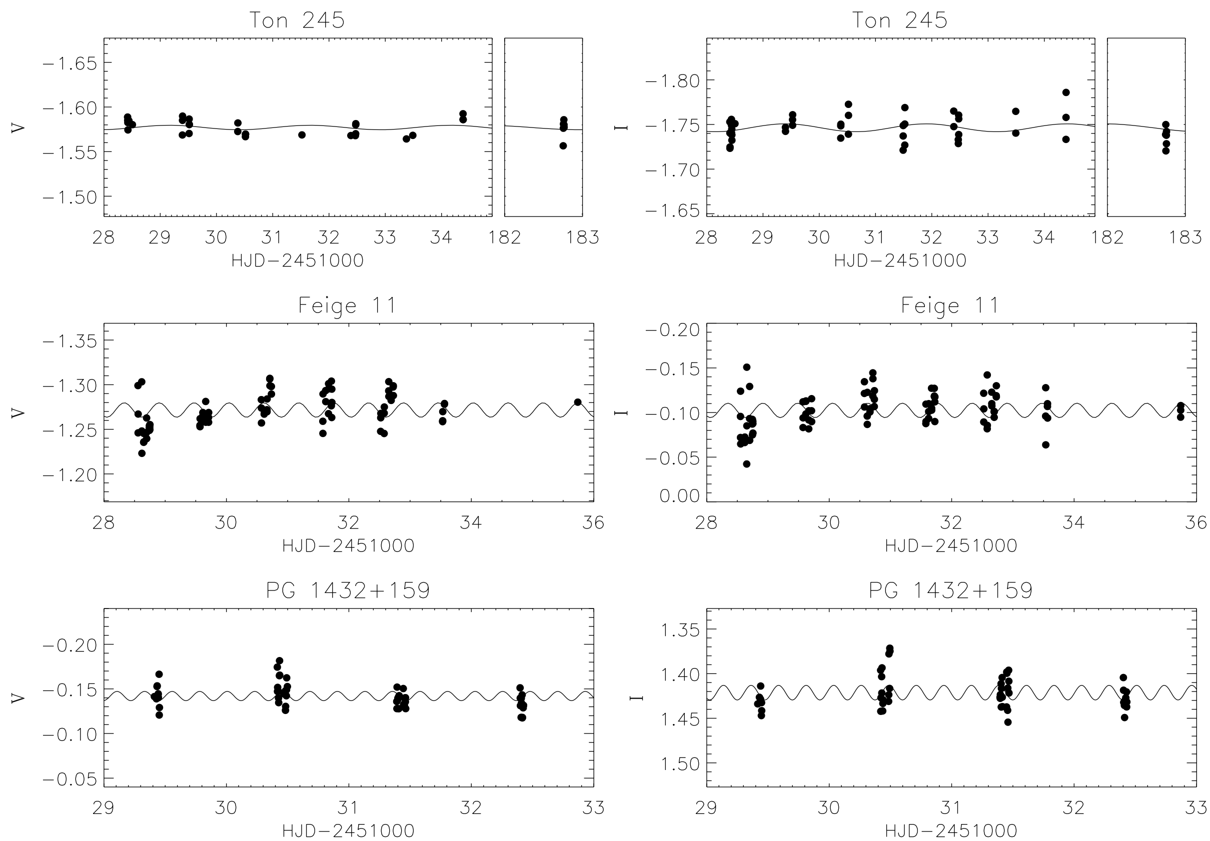

Table 6. Parameters of Ton 245, Feige 11 and PG 1432+159. The effective temperature ($T_{\rm eff}$) and surface gravity ($\log g$) are taken from Saffer et al. (1994). $M_{\rm min}$ is the minimum mass of the companion assuming a mass of $0.5M_{\odot}$ for the sdB star and $\delta m_{\rm min}$ is the minimum amplitude of the reflection effect expected from a main-sequence companion given the upper limit to the luminosity ratio $L_{\rm max}$.

Name	$T_{\rm eff}$ (K)	$\log g$ (cgs)	P (d)	K ($\rm km\,s^{-1}$)	$M_{\rm min}$ ($M_{\odot}$)	$L_{\rm max}$	$\delta m_{\rm min}$ V	$\delta m_{\rm min}$ I	Ref.
Ton 245	25200	5.30	2.5	75	0.47	0.0046	0.05	0.12	Foss, Wade & Green, 1991
Feige 11	28400	5.63	0.569908	104.3	0.37	0.0026	0.29	0.53	Moran et al., 1999
PG 1432+159	26900	5.75	0.2249	120.0	0.30	0.009	0.44	0.65	Moran et al., 1999

REFERENCES

Caillault J.-P., Patterson J., 1990, AJ, 100, 825

d'Cruz N.L., Dorman B., Rood R.T., O'Connell R. W., 1996, ApJ, 466, 359.

Downes R.A., 1986, ApJS, 61, 569.

Drechsel H., Heber U., Napiwotzki R., Østensen R., Solheim J.-E., Johannessen F., Schuh S.L., Deetjen J., Zola S., 2001, A&A, 379, 893.

Foss D., Wade R.A., Green R.F., 1991, ApJ, 374, 281.

Green R.F., Schmidt M., Liebert J., 1986, ApJS, 61, 305.

Heber U., 1986, A&A 155, 33.

Hilditch R.W., Harries T.J., Hill G., 1996, MNRAS, 279, 1380.

Hill G., Rucinski, S.M., in Milone E.C., ed., Lightcurve Modeling of Eclipsing Binary stars. Springer-Verlag, Berlin, p.135.

Iben I., Livio M., 1993, PASP, 105, 1373.

Iriarte B., 1959, Lowell Obs. Bull., 4, 130.

Kilkenny D., O'Donoghue D., Koen C., Stobie R.S., Chen A., 1997, MNRAS, 287, 867

Kilkenny D., O'Donoghue D., Koen C., Lynas-Gray A.E., van Wyk F., 1998, MNRAS 296, 329.

Kiss L.L., Csák B., Szatmáry,K., Furész G., Sziládi K., 2000, A&A, 364, 199.

Koen C., Orosz J.A., Wade R.A., 1998, MNRAS, 300, 695.

Koen C., O'Donoghue D., Pollacco D.L., Charpinet S., 1999, MNRAS, 305, 28.

Landolt, A.U., 1983, AJ, 88, 439.

Oke J.B., 1990, AJ, 99, 1621

Marsh, T.R., 1989, PASP 101, 1032.

Maxted P.F.L., Heber, U., Marsh T.R., North R.C., 2001, MNRAS, 326, 1391.

Maxted P.F.L., Marsh T.R., North R.C., 2000, MNRAS, 317, L41.

Moran C., Maxted P., Marsh T.R., Saffer R.A., Livio, M. 1999, MNRAS, 304, 535.

Napiwotzki R., 1997, A&A, 322, 256

Naylor, T., 1998, MNRAS, 296, 339

Pollacco D.L., Bell S.A., 1994, MNRAS, 267, 452.

Saffer R.A., Bergeron P., Koester D., Liebert J., 1994, ApJ, 432,

Figure 6. The amplitude of the reflection effect, δm, predicted by our model in V (solid line) and I (dashed line) and the luminosity ratio in the V band, L_V, as a function of the inclination for a main-sequence companion.

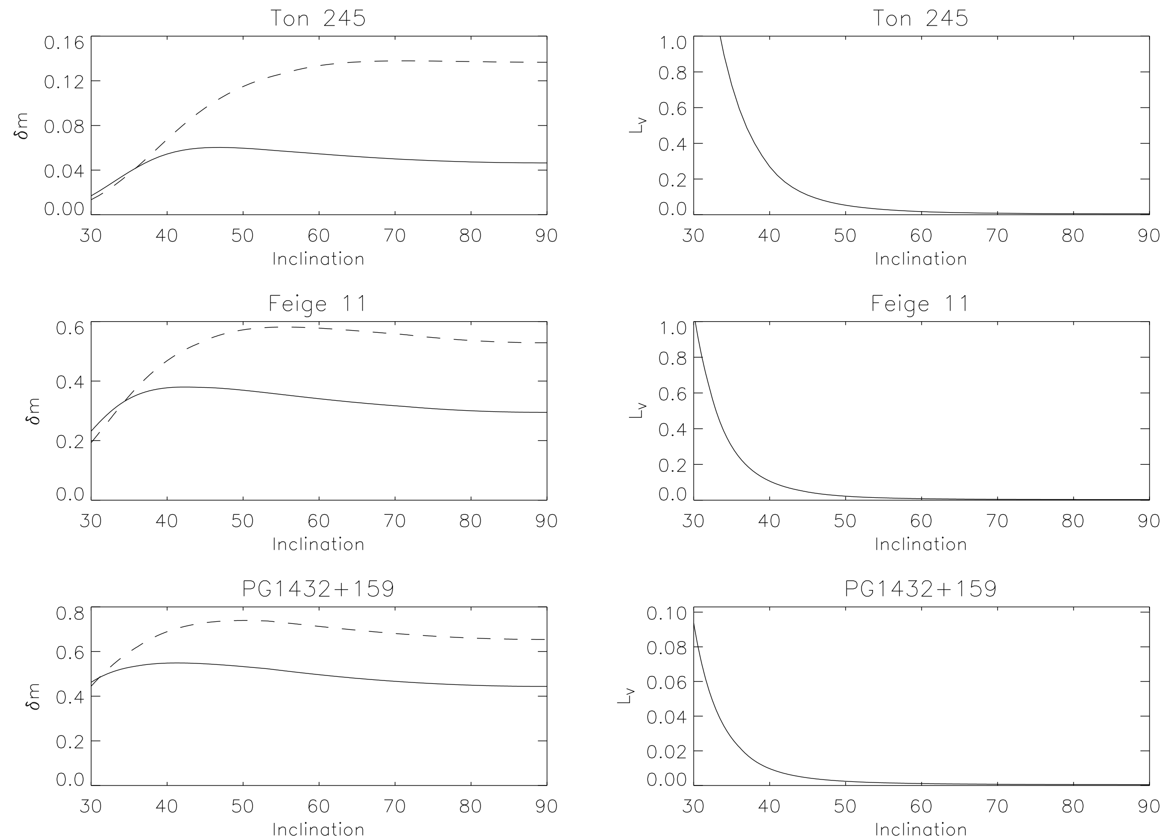

351.
Wesemael F., Fontaine G., Bergeron P., Lamontagne R, Green R.F. 1992, AJ 104, 203
Wilson R.E., Devinney E.J., 1971, ApJ, 166, 605.
Wood J.H., Zhang E.H., Robinson E.L., 1993, MNRAS, 261, 103.
Wood J.H., Saffer R., 1999, MNRAS, 305, 820.
Zombeck M.V., 1990, Handbook of Space Astronomy and Astrophysics, Second Edition, Cambridge University Press, Cambridge, UK.

Figure 7. Periodograms of our V and I lightcurves for Ton 245, Feige 11 and PG 1432+159. The orbital frequency is marked with a dashed vertical line. The short horizontal line marks the minimum semi-amplitude expected for a non-degenerate companion, $\delta m_{\rm min}/2$.